Please cite the final version:
N. George. P. Ripka: Rectangular Busbar with Circular Sensing Part for Wideband Current Measurement,
IEEE Trans. Instr. Meas. 72, 9509008. doi 10.1109/TIM.2023.3289559

Rectangular Busbar with Circular Sensing Part for Wideband Current Measurement

Noby George, and Pavel Ripka

***Abstract*— A simple, reliable and novel busbar sensing configuration for frequency-independent current measurement is presented in this paper. Yokeless current transducers using arrays of magnetic sensors around a rectangular busbar is linear and lightweight, but they suffer from large frequency dependence. Several circular-array based current transducers have been described in the literature, but their frequency characteristics have never been studied in detail. We show that the magnetic field surrounding a long circular busbar is frequency-independent, regardless of the surface effect. This feature can be used to develop an accurate circular-array based coreless Hall current transducer for a wide range of frequencies We propose a novel busbar configuration that has a 200 mm long circular section in the current-sensing part of the busbar, and which is compatible with the standard 10 × 60 mm rectangular busbar. A circular magnetic field sensor array is mounted in the midplane, around the circular conductor, for the current measurement. A Finite Element Method (FEM)-based 3-D analysis of the proposed busbar is performed with the help of an eddy current solver in the Ansys Maxwell tool. In addition, a prototype of the proposed wideband busbar was developed in the laboratory and its functionality was tested. The results that have been obtained show that the frequency dependence is reduced from -8.5% (for a rectangular busbar) to -0.45% (for the novel transducer).**

***Index Terms*—Busbar current sensor, yokeless current measurement, eddy current effect, Hall sensor array.**

I. Introduction

Yokeless current transducers based on a circular array of magnetic field sensors are used for DC and AC current measurement in the mA to kA range [1]-[4]. Since no magnetic core is used, these methods do not suffer from the non-idealities of the magnetic core. Current Transformers are in use to measure AC currents. They have many limitations including the errors due to magnetic saturation [5]. The air gapped magnetic core current transducer with Hall-Effect sensor placed in the gap [1] measure both DC and AC currents, but the necessity of the airgap causes unwanted sensitivity to external magnetic fields and to the position of the measured conductor. The yokeless circular array-based transducers are simple, lightweight, and can be made resistant to the effect of external magnetic fields [6]. Mostly, these are meant for power frequency measurement. Various factors, e.g. the crosstalk effect [7], [8], and misalignment of the sensing elements or of the conductor [9]-[13], which affect the performance of yokeless current transducers, are well studied in the literature. Along with the factors mentioned above, it is important to study the frequency characteristics of yokeless current transducers. Wide-band current measurements are necessary in power electronic converters such as solar inverters, motor drives, and uninterrupted power supplies [14], [15]. Yokeless current transducers based on a circular array of magnetic sensors are widely used. As far as we know, no through investigation of the frequency dependency of this transducer has been reported in the literature.

A circular/elliptical array of magnetic sensors is also used for measuring current in rectangular busbar conductors [16], [17], but these transducers are highly frequency-dependent due to the skin effect. The frequency compensation of rectangular busbar current transducers is accomplished with the help of digital filters [18], sensor position optimization algorithms [19], and structural modifications to the rectangular shape [20], [21]. The design of digital filters requires simulation studies to finalize the locations of sensors in the rectangular array and to design filters for each of the sensors in the array [18]. Digital filters also introduce phase errors. Xu et al. have found points with low-frequency dependence in the vicinity of a rectangular conductor. They achieved 1.5 % frequency dependence at 1 kHz [19]. A problem with their design is limited suppression of external fields [7]. A rectangular busbar with a hole in the middle helps to position differential sensors in the hole and to adjust the sensitivity of the transducer to fit the required current range [20]. An amphitheater structure [21] for the hole and an asymmetrical structure for the busbar [20] help to reduce the error at 1kHz to 9% for the amphitheater hole and ±3% for the asymmetrical busbar structure.

In this paper, the frequency dependency of the magnetic field surrounding a long circular busbar is studied and the results are presented for the first time. It is shown that the magnetic field surrounding an infinitely long circular busbar is frequency-independent. 3D Finite Element Method (FEM)-based

This paragraph of the first footnote will contain the date on which you submitted your paper for review. Noby George is supported by International mobility of research, technical and administrative staff of research organizations, “CZ.02.2.69/0.0/0.0/18_053/0016980.”

Noby George is with the Faculty of Electrical Engineering, Czech Technical University, Prague, Czech Republic, (e-mail: noby.george@fel.cvut.cz).

Pavel Ripka is with the Faculty of Electrical Engineering, Czech Technical University, Prague, Czech Republic, (e-mail: ripka@fel.cvut.cz).

analytical and experimental studies were performed to find how the situation changes for a circular conductor section of finite length. The frequency independence of the magnetic field of a circular busbar is utilized to develop a novel and simple structure for a rectangular busbar with a circular current-sensing part. A circular array of 8 Hall magnetic field sensors is used in the circular sensing part of the busbar for wide frequency current measurements up to 1 kHz. The new aspects of the proposed wideband busbar current transducer presented in this paper are summarized below.

- We show that if we use the yokeless circular array-based current transducer, positioned at the circular current sensing part of the proposed busbar current transducer, the current measurement will be independent of the frequency of the current in the busbar.
- We show that for a circular busbar part with sufficient length, due to the circular symmetry, the magnetic flux density around it is frequency-independent, i.e., not affected by the skin effect in the bus bar. This is proven with the help of finite element analysis, and experimental results.
- Experimental results are presented to show the frequency dependency of the magnetic fields around circular and rectangular busbar conductors. Such measurement results are not reported before to our knowledge.
- The accuracy of the prototype built based on the proposed approach is -0.45 % at 1 kHz. This is much better than the other frequency compensation based on geometrical modifications such as for amphitheater [21] (9 % at 1 kHz) and wedge-shape [20] structures (±3 % at 1 kHz). Also, the proposed wideband transducer is simple and reliable as it does not require digital filters [18] or position optimization algorithms leading to reduced rejection of external currents [19].
- The proposed design ensures that the current carrying capacity of the busbar is not altered.
- The proposed wideband configuration helps to reduce frequency dependency for higher frequencies also (more than 1 kHz).

This paper is organized as follows. The frequency independency of the magnetic field around a long circular busbar is proven in section II. Details about the structure of the proposed wideband busbar, the arrangement of a circular array of sensors in the current-sensing part of the busbar, and related FEM results, are provided in section III of the paper. A detailed experimental and FEM analysis of the proposed wideband configuration is carried out and results are provided in section IV. Section V provides a comparison of the features, which is followed by a conclusion.

II. The Frequency Dependency of a Circular Busbar and a Rectangular Busbar

A. Frequency Dependency of the Magnetic Field in a Circular Busbar

Yokeless current transducers based on an array of magnetic sensors measure the tangential component of the flux density (*B*) around a current-carrying conductor/busbar and calculate the respective current in the conductor [22]. It is important to study the behavior of *B* around a circular busbar at different frequencies. Ampere's circuital law provides the value of *B* outside a conductor, according to (1).

$$\oint B.dl = \mu_0 I \tag{1}$$

In (1), I is the total current enclosed by the integration line, and μ_0 is the permeability of the free space ($4\pi\times10^{-7}$).

This equation is valid for arbitrary shape of the conductor and for an arbitrary closed integration line. If the conductor is circular and the integration path is a concentric circle with radius *r*, at each point of that circle *B* will have the same value of

$$B = \frac{\mu_0 I}{2\pi r} \tag{2}$$

This equation is well known and evident because of the symmetry. If the conductor is not circular, (1) is still valid, but the symmetry is broken and *B* is no longer constant.

It is well known that at higher frequencies the current in a massive conductor is no longer homogeneous, due to the surface effect caused by eddy currents. However, due to the symmetry, (2) will remain valid for circular conductors.

It is therefore clear that the flux density outside an infinitely long circular conductor does not vary with the frequency of the current in the conductor. The same can be verified for finite length circular busbar using FEM analysis.

B. Frequency Dependency of the Magnetic Field in a Rectangular Busbar

A circular array with right offset angle for the sensors is presented in [23] for the measurement of current in a rectangular busbar. The work presented in [17] suggests an elliptical sensor array to measure the current in rectangular busbar. These two configurations help reduce the effect of shape of the rectangular conductor, and the frequency response of such kind of configurations is not studied in detail. The non-uniform nature of the magnetic field around rectangular busbar is already mentioned in the literature [18]- [21]. An analysis in this direction is provided in the next section of the paper.

III. The Wideband Busbar Configuration and the Circular Array of Sensors

A novel busbar configuration that allows wideband current measurement in massive conductors is shown in this paper. The proposed busbar configuration makes use of the property of an infinitely long circular busbar that the magnetic flux density around it is frequency-independent (as presented in *section II. A*). To achieve the wideband property, a long circular busbar portion (with a comparable cross-sectional area) is inserted into a standard 10x60 mm rectangular busbar. The circular busbar portion is 30 mm in diameter and 200 mm in length. Details of the dimensions of the proposed wideband busbar transducer are provided in Fig.1a.

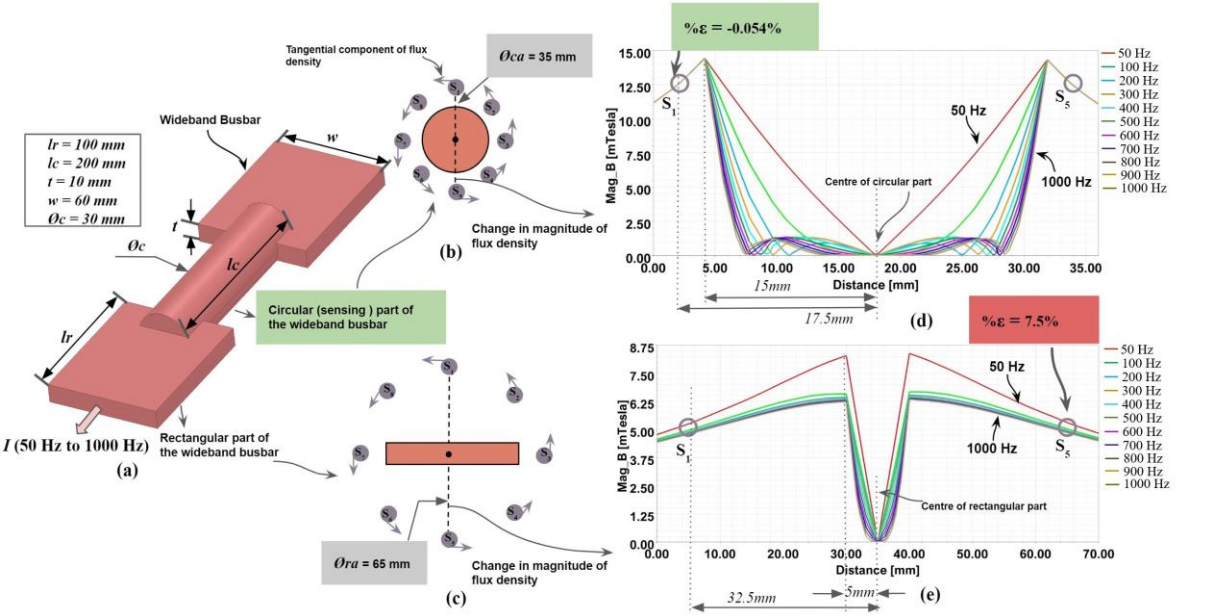

Fig. 1a. The wideband busbar with circular sensing part. The circular array of 8 magnetic field sensors is arranged around (b) circular and (c) rectangular part of the busbar for comparison. The frequency dependency of (d) circular sensing part is lower compared to the (e) rectangular part in the busbar. The relative error (% Ɛ) at the sensor position 1 or 5 is -0.054 % for circular, and 7.5 % for rectangular part.

A 3D model (shown in Fig.1a.) of the wideband busbar transducer is developed in the Ansys Maxwell tool and its frequency characteristics are analyzed using the eddy current solver. During FEM analysis, the current through the wideband copper busbar is kept constant at 1000 A and the frequency is varied from 50 Hz to 1000 Hz. A circular array of 8 sensors (S_1 and S_8) is used in the circular part of the busbar. The magnitude of flux density (the output voltage of the sensor in the case of experimental analysis) at the 8 sensor locations is averaged to study the frequency dependency along with analyzing the frequency dependency at individual sensor locations of the array. The diameter of the sensor array for the circular current sensing part of the busbar is chosen to be 35mm (shown in Fig.1b.). Also, a sensor array with a 65 mm diameter is considered for the rectangular part of the busbar (shown in Fig. 1c.) to study its frequency characteristics.

The change in the magnitude of the flux density through a line passing through the center of the circular busbar and connecting sensors S_1 and S_5 is shown in Fig. 1d. Fig.1d shows that the flux density at the sensor locations (marked as S_1 and S_5) is frequency-independent. Also, it is evident from Fig.1d. that the magnitude of the flux density is different for different frequencies inside the circular busbar portion, but it is same for different frequencies outside the circular busbar portion. The magnetic flux densities at the other sensor locations also follow similar characteristics due to the symmetric structure of the circular busbar. A detailed analysis of the frequency characteristics at each of the sensor locations is provided in the next section of the paper.

The frequency dependency of the magnetic field around rectangular busbar, and the sensor array is provided in Fig.1e. Fig. 1e. shows that the magnitude of the flux density at the sensor locations (marked as S_1 and S_5) is different for different frequencies outside the rectangular part of the busbar. The frequency dependency at the other sensor locations (other than S_1 and S_5) is different in the case of the rectangular busbar, due to its asymmetric structure. The relative error calculated by considering the frequency dependence at all the sensor locations, when a rectangular bar is used, is -8.5%. This study was conducted at 1 kHz.

The proposed configuration of the busbar can be used for the wideband current measurement by keeping the widely-used circular array of magnetic sensors in the circular sensing part of the busbar. A circular array of sensors can be realized by placing 8 suitable magnetic field sensing elements. A block diagram representation of the proposed busbar configuration and a circular array of sensors is provided in Fig. 2. The output voltages from 8 sensors are averaged using the summing amplifier [22]. Along with V_{out}, the frequency characteristics of the output voltage from each of the sensors (V_1 to V_8) are also analyzed in this paper. A detailed analysis of the frequency characteristics of the proposed busbar configuration is provided in the next section of the paper.

IV. An Experimental Analysis and an FEM-Based Analysis of the Wideband Configuration

A detailed analysis of the proposed busbar configuration to check its ability to measure large bandwidth current is presented in this section. The experimental analysis is performed in the laboratory using the prototype of the busbar transducer and a circular array of sensors. The eddy current solver in the Ansys Maxwell tool is used for the FEM analysis with the help of a 3D model of the wideband busbar.

A. The Prototype of the Wideband Busbar Transducer and a Circular Array of Sensors

A prototype of the wideband busbar (dimensions given in Fig. 1a.) was developed in our laboratory and its frequency dependency was tested. The busbar is made of copper and a

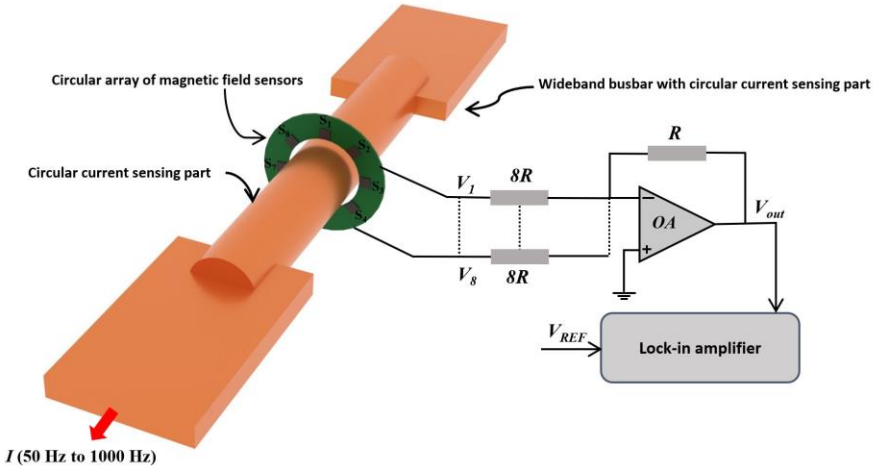

Fig. 2. A block diagram representation of the proposed wideband busbar configuration and arrangement of circular array of sensors. A summing amplifier is used to get the average of the output voltages of the sensors in the array, and a lock-in amplifier is used to study the frequency characteristics.

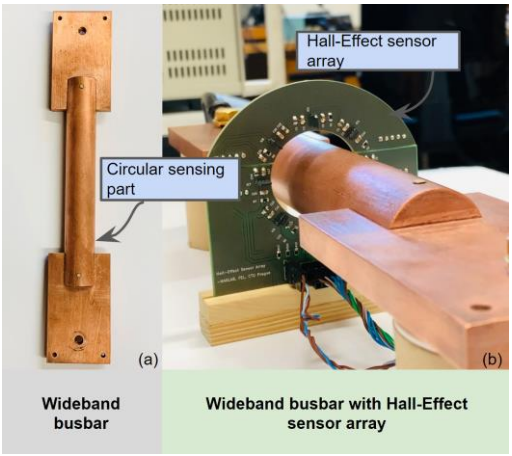

Fig. 3a. The wideband copper busbar transducer developed at our laboratory. The Hall-Effect sensor array (b) along with summing amplifier is designed in a printed circuit board and it is mounted in the circular current sensing part of the wideband busbar.

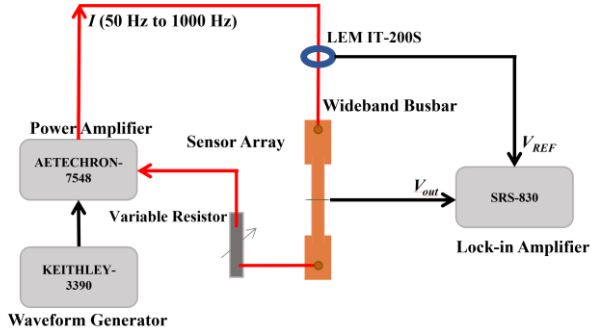

Fig. 4. A block diagram representation of the measurement system used for analysing the frequency characteristics of the proposed wideband busbar and circular array of sensors.

picture of the developed busbar is provided in Fig. 3a. The circular array of 8 sensors can be realized using magnetic field sensing elements with a suitable bandwidth and sensing range. Hall-effect based magnetic field sensors are used in the prototype of the array of sensors. The Melexis Technologies MLX91209 Hall sensors [24] have a bandwidth up to 250 kHz, a sensing range of ±150mT, linearity error of 0.4%, and sensitivity of 150 mV/mT. An array of MLX91209 Hall-Effect sensors developed in our laboratory is shown in Fig.3b. The supply voltage (V_{dd}) of the MLX91209 is 5V. The diameter of the sensor array is 35 mm.

B. Measurement System

A suitable measurement and signal conditioning system that can analyze the frequency characteristics of the proposed busbar and Hall sensor array was developed in the laboratory. A block diagram representation of the measurement system is shown in Fig.4. The average value of the output voltages of the 8 Hall sensors in the array is obtained using a summing amplifier (as shown in Fig.3) using an Analog Devices Inc. ADA4075 low-noise operational amplifier. The output voltage of the summing amplifier at each frequency is measured using a Stanford Research Systems SR830 lock-in amplifier. The SR830 displays both the magnitude and the phase of the input signal. The reference signal bandwidth of the SR830 is 102.4 kHz. The Keithley 3390 arbitrary waveform generator along with an AE Techron Inc. 7548 power amplifier is used to pass different sine wave current frequencies (50 Hz to 1 kHz) through the wideband busbar. The measurement system that is used is intended to study the frequency characteristics of the proposed wideband busbar. For industrial applications, the V_{out} from the summing amplifier can be digitized using suitable Analog to Digital Converters (ADC) or Data Acquisition Systems (DAS), and the current can be calculated using (2) [22], [25].

C. Frequency Characteristics of the Wideband Transducer

In order to test the frequency characteristics of the proposed wideband transducer, the frequency of the current (constant) through the wideband busbar is varied from 50 Hz to 1000 Hz

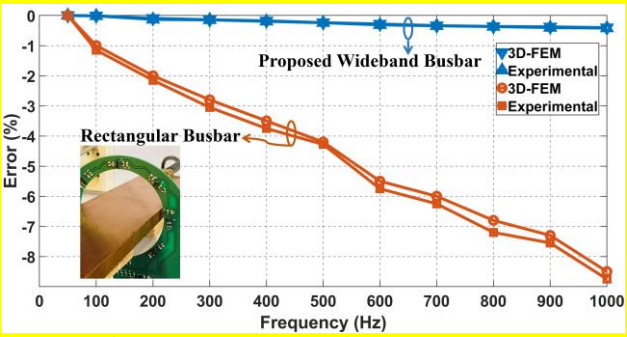

Fig. 5. The frequency characteristics of the proposed wideband busbar current transducer . The plot also shows the characteristic when the conventional rectangular busbar is used. A picture of the conventional rectangular busbar and circular array of sensors is shown in the inset.

(maximum frequency obtained using the measurement setup provided in Fig. 4), in steps of 100 Hz. The Hall sensor array was kept within the circular sensing part of the busbar during the test. The frequency characteristics of the proposed busbar

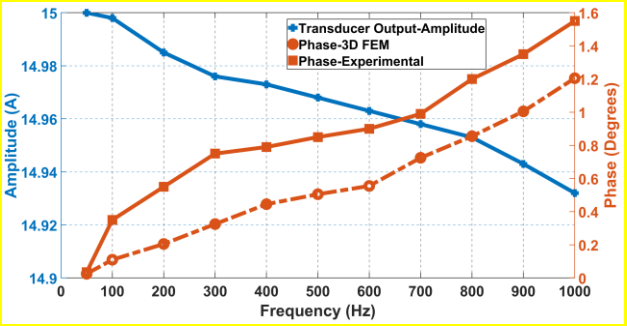

Fig. 6. The amplitude and phase (experimental and FEM) versus frequency characteristics of proposed wideband busbar transducer.

current transducer are analysed by checking the output of the summing amplifier (V_{out}), at different frequencies, using the lock-in amplifier. The relative error at each frequency is calculated using (3)

$$\%Error = \frac{V_{out(50Hz)} - V_{out(f)}}{V_{out(50Hz)}} \times 100 \qquad (3)$$

A suitable prototype, using a Hall-Effect sensor array, has been developed to measure the current in a 60×10 mm rectangular busbar. The circular array has a diameter of 65 mm. The experimental and 3D-FEM results showing the comparison of frequency characteristics of the proposed wideband current measurement approach and the conventional rectangular busbar approach are provided in Fig. 5. The maximum error observed for the proposed wideband busbar is -0.45%, which is much better than -8.5 % noted we use a rectangular busbar. Both tests were done at 1 kHz. The current through the wideband busbar was kept constant at 15 A (maximum current provided by the measurement setup in Fig. 4 at 1 kHz) during the frequency dependency analysis. The measured current is calculated from V_{out} using (1) and the change in amplitude of current measured by the proposed transducer for a frequency range up to 1 kHz is provided in Fig. 6. The phase error of the proposed wideband busbar is also provided in Fig. 6. The current sensor LEM IT-200S is used as a reference for phase measurement.

The effect of the length of the circular sensing part in the wideband busbar is studied using 3D-FEM. The length of the circular sensing part was changed from 200 mm to 300 mm, and 100 mm (with all other dimensions the same), and the corresponding frequency characteristics are provided in Fig. 7.

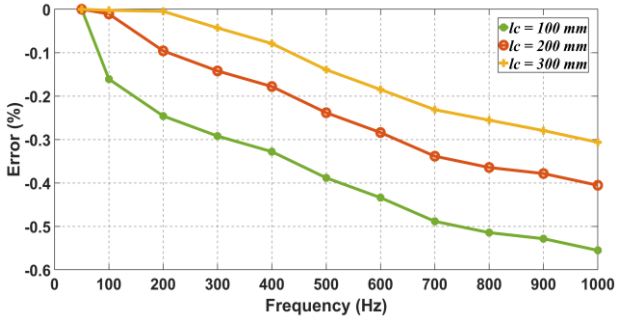

Fig. 7. The effect of change in length of the circular current sensing part on the final accuracy (associated with frequency) of the current measurement.

The results show that the circular sensing part must be sufficiently long for the frequency-independent measurements. As expected, longer the length of the circular part, the accuracy is higher. For the detailed studies, we used the circular part with 200 mm which is 3 times the width of the flat busbar.

D. Frequency Characteristics of Individual Sensors in the Hall Sensor Array

Magnetic sensor based yokeless current transducers mostly use 8 sensors in the array, since such array is highly immune to external fields [7]. The frequency characteristics of all 8 Hall sensors (as marked in Fig.1b) in the array are studied individually, and the results are provided in Fig.8, and in Fig.9.

Hall sensors S_1, S_3, S_5, and S_7 exhibit lower frequency

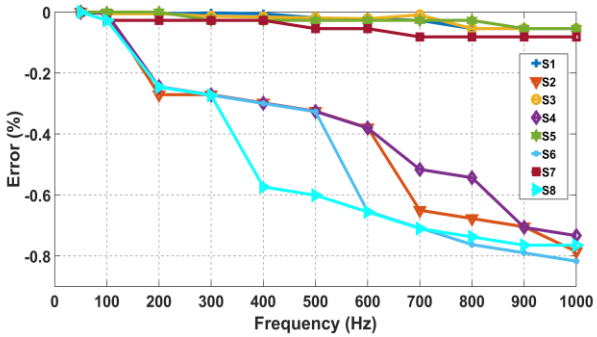

Fig. 8. The frequency characteristics of individual sensors in the array (experimental results).

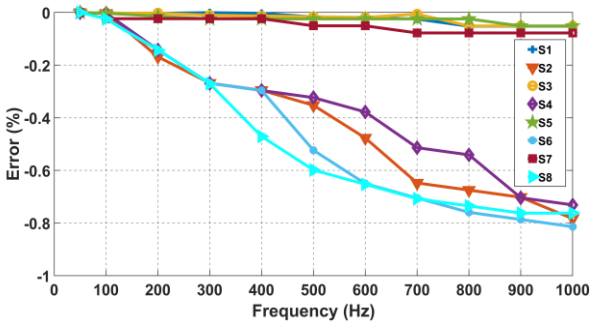

Fig. 9. The frequency characteristics of individual sensors in the array (3D-FEM results).

dependency, and the maximum error noted is - 0.0813% (for S7 at 1 kHz). Hall sensors S_2, S_4, S_6, and S_8 which are diagonally placed in the array show high frequency dependency, and the maximum error is 0.8172% (for S_6 at 1 kHz). The reason for this interesting effect is the influence of the eddy currents from the distant rectangular part of the busbar. Sensors S_1, S_3, S_5, and S_7 are located in the symmetry planes, and they are less affected by these currents.

The frequency characteristics of each of the sensors are also obtained using the 3D FEM-based study, and the results are provided in Fig.9. The analysis of each of the sensors showed that it is possible to reduce the frequency dependency of the proposed transducer further by using only 4 Hall sensors (at locations 1, 3, 5, and 7 marked in Fig. 1b). The Hall sensor array formed using the 4 sensors S1, S3, S5, and S7 showed -0.0516% error at 1 kHz.

E. Experimental Analysis of the Wideband Transducer for Large Current and Frequency Ranges

The experimental analysis of the proposed wideband busbar for large current and frequency ranges is presented in this section. The measurement setup provided in Fig. 4 is modified as in Fig. 10 to pass wide ranges of current and frequency through the proposed transducer. In the modified setup, the output of the power amplifier is connected to the secondary side of a 2000 VA, 50 Hz Current Transformer (CT), and the primary of the CT is shorted through the wideband transducer using proper cables. The power amplifier is operated in constant voltage mode and two cables are connected in parallel in the primary of the CT to reduce the impedance. This provided up to 1 kA current at 50 Hz, and up to 20 A at 4 kHz. The actual current is measured using the LEM IT-1000 S current sensor with an accuracy of 0.0054 %. Initially, the current through the wideband busbar is varied from 0 to 1000 A, in steps of 100 A at 50 Hz, and the output of the transducer (V_{out}) is measured using a lock-in amplifier. The V_{out} changed linearly with the measured current as shown in Fig 11. The maximum linearity error noted is 0.31 % of the full scale. In the next analysis, the current through the wideband busbar is fixed at 20 A and the frequency of the current is varied from 50 Hz to 4 kHz. The measured relative error is provided in Fig. 12, and the maximum relative error noted is - 0.698 % at 4 kHz.

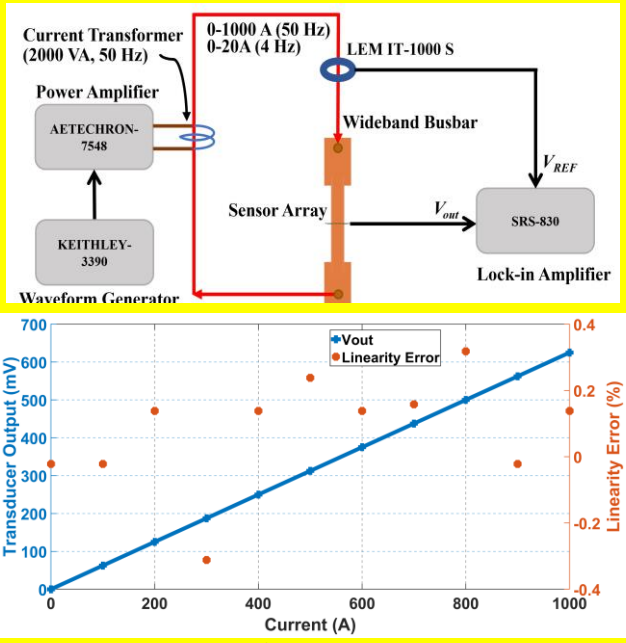

Fig. 11. The measurement of current up to 1 kA using the proposed wideband transducer.

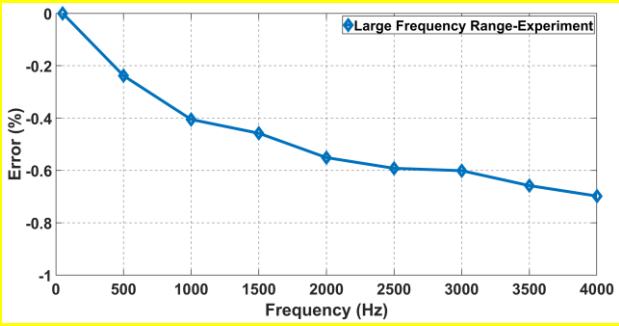

Fig. 12. The frequency dependency of the proposed wideband transducer for a frequency range up to 4 kHz.

F. Effect of a nearby Busbar on the proposed Wideband Transducer

The effect of a nearby current-carrying busbar on the wideband current transducer is presented in this section. The immunity of a circular array of sensors with 8 sensing elements was examined in [7], only for low frequncies. In this paper, we analyze this influence for frequencies up to 1 kHz. The standard rectangular busbar (Fig. 13a) and a wideband busbar (Fig. 13b) are kept at a distance d = 125mm from the proposed busbar, and 3D-FEM analysis is carried out in two different cases. The frequency of the current through the proposed wideband busbar also varied from 50 Hz to 1000Hz during the test. The relative error at each sensor location for a rectangular busbar interference is presented in Fig. 14 (rectangular and wideband busbar interference showed similar results). The FEM analysis is verified using an experimental test by keeping a rectangular busbar near (d =125mm) to the proposed wideband busbar, as shown in Fig. 15. The frequency characteristics at each sensor location during the experimental test are presented in Fig. 16. The relative error at each sensor location (other than S_1 and S_5) is high, as expected. As these errors have different signs, they partly compensate, and the relative error of V_{out} is only 0.82% during the FEM study and 1.03% during the

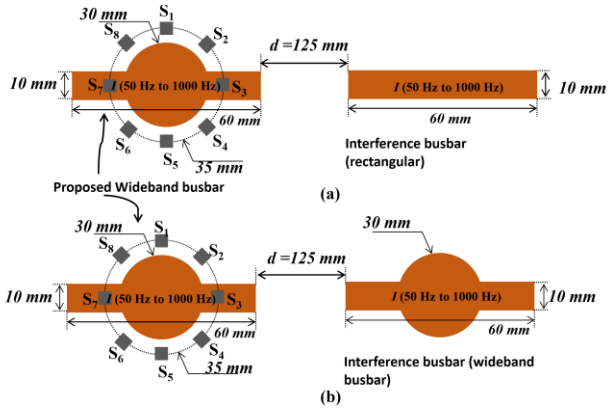

Fig. 13a. A rectangular, and (b) wideband interference busbars near the proposed wideband busbar.

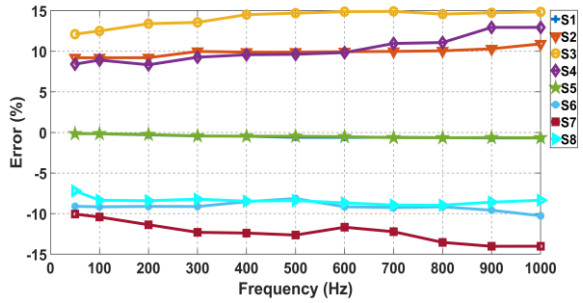

Fig. 14. The frequency characteristics of individual sensors in the array with rectangular busbar interference (3D-FEM results).

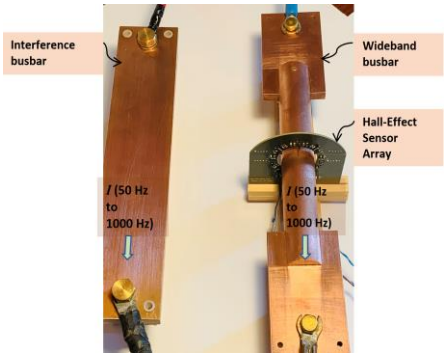

Fig. 15. The rectangular interference near the proposed wideband busbar during the experimental analysis.

experimental study, at 1 kHz. This is similar to the operation of the gradient sensor, which is completely immune against the homogeneous field. The frequency characteristics of the proposed wideband busbar transducer with an interference rectangular busbar are shown in Fig. 17. Distance *d* was kept at 125 mm during this test, as this is the minimum safe clearance distance in standard high voltage systems [18].

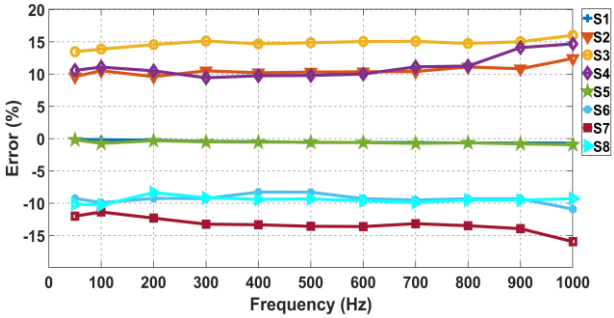

Fig. 16. The frequency characteristics of individual sensors in the array with rectangular busbar interference (experimental results).

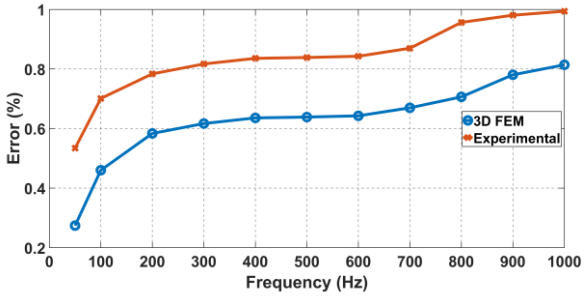

Fig. 17. The frequency characteristics of the proposed wideband busbar with rectangular busbar interference.

V. Comparison of Features and Discussion

The features of the proposed wideband busbar current transducer are compared with the existing frequency compensation techniques for wideband busbar current measurements, and are provided in Table I. Busbar with modified shapes are reported to improve the frequency range but the current carrying capacity of the bus bar is reduced [20]-[21]. Other methods require sensor position optimization

TABLE I
Comparison of Features

Frequency compensation technique	Uses circular array of sensors	Affects current carrying capacity	Type of magnetic field sensor	Complexity	Position optimization required	Frequency Range	Maximum relative error
Amphitheater busbar structure [21]	No	Yes	Fluxgate	Less	Yes	1 kHz	9 %
Wedge shape busbar structure [20]	No	Yes	Fluxgate	Less	Yes	1 kHz	±3 %
Digital filter [18]	No	No	Hall-Effect	High	Yes	2.5 kHz	1 %
Position Optimization algorithm [19]	No	No	TMR	High	Yes	1 kHz	1.5 %
This paper (wideband busbar configuration)	Yes	No	Hall-Effect	Very Less	No	1 kHz[#]	-0.45 % for 8 sensors[*] -0.05 % for 4 sensors[*]

Note: [*] This is achieved due to the proposed configuration.
[#] The frequency range can be increased (since the flux density values outside the current sensing part of the busbar, for the same current, is the same for all frequencies).

algorithms [19], use of specially tuned digital filters [18], etc. It is evident from Fig.1d. that the flux density values outside the busbar, for the same current, is same for all frequencies. The same is verified by the experimental studies. We did a 3D-FEM analysis for a frequency range of up to 10 kHz. The error observed was less than 0.9 %. The Hall-Effect sensor used in the prototype circular array has a bandwidth of up to 250 kHz [24]. Hence the prototype sensor can sense flux density values up to 250 kHz.

The proposed technique is also simple and reliable since it requires only incorporating the sufficiently long circular sensing part in a rectangular busbar without affecting the current carrying capacity. The manufacturing of the proposed configuration is less complicated compared to the existing busbar geometry modification-based approaches [20]-[21].Widely-used circular array sensors can be used in the proposed wideband configuration for frequency-independent current measurement, but this not possible in any available compensation technique. A circular array of sensors helps to reduce the effect of external magnetic fields.

VI. Conclusion

The analytical, FEM, and experimental study presented in this paper has shown that the magnetic flux density around an infinitely long circular busbar is frequency independent. This property is used to develop a wideband rectangular busbar current transducer with a circular sensing section. A Hall-based yokeless current transducer is used in the circular part of the busbar for frequency-independent current measurements. The frequency dependency of a rectangular busbar using an array of Hall sensors can be reduced from 8.5% to -0.45% at 1 kHz, using the proposed busbar configuration. The Hall sensor array using 4 sensors (S1, S3, S5, and S7) showed a -0.05 % error at 1 kHz, which is better than the - 0.45% error at 1 kHz for 8 Hall sensors in an array. However, an 8-sensor array has better suppression of external currents [7]. The effect of the nearby current-carrying busbar only slightly increasing with frequency, reaching 1% error at 1 kHz for 125 mm distance.

References

[1] P. Ripka, “Electric current sensors: A review,” *Meas. Sci. Technol.*,vol. 21, no. 11, pp. 1–23, Sep. 2010.

[2] J. Li, H. Liu and T. Bi, "Tunnel Magnetoresistance-Based Noncontact Current Sensing and Measurement Method," *IEEE Trans. Instrum. Meas.*, vol. 71, pp. 1-9, 2022.

[3] G. Geng, J. Wang, K. -L. Chen and W. Xu, "Contactless Current Measurement for Enclosed Multiconductor Systems Based on Sensor Array," *IEEE Trans. Instrum. Meas.*, vol. 66, no. 10, pp. 2627-2637, Oct. 2017.

[4] X. Liu, W. He, Y. Zhao, Y. Guo and Z. Xu, "Nonintrusive Current Sensing for Multicore Cables Considering Inclination With Magnetic Field Measurement," *IEEE Trans. Instrum. Meas.*, vol. 70, pp. 1-14, 2021.

[5] M. Davarpanah, R. Iravani and M. Sanaye-Pasand, "A saturation suppression approach for the current transformer—Part II: Performance evaluation", *IEEE Trans. Power Del.*, vol. 28, no. 3, pp. 1936-1943, Jul. 2013.

[6] P. Mlejnek, M. Vopálenský, P. Ripka: AMR current measurement device, Sens. Act. A 141, pp. 649-653, 2008.

[7] R. Weiss, R. Makuch, A. Itzke and R. Weigel, "Crosstalk in circular arrays of magnetic sensors for current measurement", *IEEE Trans. Ind. Electron.*, vol. 64, no. 6, pp. 4903-4909, Jun. 2017.

[8] A. Itzke, R. Weiss, T. DiLeo and R. Weigel, "The influence of interference sources on a magnetic field-based current sensor for multiconductor measurement", *IEEE Sensors J.*, vol. 18, no. 16, pp. 6782-6787, Aug. 2018.

[9] X. Ma, Y. Guo, X. Chen, Y. Xiang and K.-L. Chen, "Impact of coreless current transformer position on current measurement", *IEEE Trans. Instrum. Meas.*, vol. 68, no. 10, pp. 3801-3809, Oct. 2019.

[10] N. George and S. Gopalakrishna, "Detailed study on error characteristics of core-less hall current transducer," *2017 Eleventh International Conference on Sensing Technology (ICST)*, 2017.

[11] J. Y. C. Chan, N. C. F. Tse and L. L. Lai, "A coreless electric current sensor with circular conductor positioning calibration", *IEEE Trans. Instrum. Meas.*, vol. 62, no. 11, pp. 2922-2928, Nov. 2013.

[12] V. Grim, P. Ripka and J. Fischer, "Characterization of circular array current transducers", *Proc. IEEE Sensors Appl. Symp. (SAS)*, vol. 21, no. 11, pp. 1-5, Mar. 2019.

[13] Xiaoyu Ma, Yi Guo, Xianan Chen, Yukai Xiang, Kun-Long Chen, "Impact of Coreless Current Transformer Position on Current Measurement", *IEEE Trans. Instrum. Meas.*, vol.68, no.10, pp.3801-3809, 2019.

[14] S. J. Nibir, M. Biglarbegian and B. Parkhideh, "A non-invasive DC-10-MHz wideband current sensor for ultra-fast current sensing in high-frequency power electronic converters", *IEEE Trans. Power Electron.*, vol. 34, no. 9, pp. 9095-9104, Sep. 2019.

[15] A. Bernieri, L. Ferrigno, M. Laracca and A. Rasile, "An AMR-Based Three-Phase Current Sensor for Smart Grid Applications," *IEEE Sensors J.*, vol. 17, no. 23, pp. 7704-7712, 1 Dec.1, 2017.

[16] L. Di Rienzo, R. Bazzocchi and A. Manara, "Circular arrays of magnetic sensors for current measurement", *IEEE Trans. Instrum. Meas.*, vol. 50, no. 5, pp. 1093-1096, 2001.

[17] R. Weiss, F. Zapf, A. Skelly and R. Weigel, "Busbar Current Measurement With Elliptical Sensor Arrays Without Conductor Specific Calibration," *IEEE Trans. Instrum. Meas.*, vol. 70, pp. 1-9, 2021.

[18] W. Li, G. Zhang, H. Zhong and Y. Geng, "A Wideband Current Transducer Based on an Array of Magnetic Field Sensors for Rectangular Busbar Current Measurement," *IEEE Trans. Instrum. Meas.*, vol. 70, pp. 1-11, 2021.

[19] X. P. Xu, S. Wang, T. Z. Liu, M. Zhu and J. G. Wang, "TMR Busbar Current Sensor With Good Frequency Characteristics," *IEEE Trans. Instrum. Meas.*, vol., vol. 70, pp. 1-9, 2021.

[20] P. Ripka, V. Grim and V. Petrucha, "A busbar current sensor with frequency compensation", *IEEE Trans. Magn.*, vol. 53, no. 4, pp. 1-5, Apr. 2017.

[21] P. Ripka, M. Přibil, V. Petrucha, V. Grim and K. Draxler, "A Fluxgate Current Sensor With an Amphitheater Busbar," *IEEE Trans. Magn.*, vol. 52, no. 7, pp. 1-4, July 2016.

[22] K. -L. Chen and N. Chen, "A New Method for Power Current Measurement Using a Coreless Hall Effect Current Transformer," *IEEE Trans. Instrum. Meas.*, vol. 60, no. 1, pp. 158-169, Jan. 2011.

[23] R. Weiss, A. Itzke and R. Weigel, "Current measurement of flat conductors with a circular array of magnetic sensors," *2017 IEEE Second International Conference on DC Microgrids (ICDCM)*, 2017, pp. 166-170, doi: 10.1109/ICDCM.2017.8001039.

[24] “Datasheet for MLX91209,” Melexis. [Online]. Available: https://www.melexis.com/en/documents/documentation/datasheets/datasheet-mlx91209.

[25] R. Weiss, A. Itzke, J. Reitenspieß, I. Hoffmann and R. Weigel, "A Novel Closed Loop Current Sensor Based on a Circular Array of Magnetic Field Sensors," *IEEE Sensors J.*, vol. 19, no. 7, pp. 2517-2524, 1 April1, 2019.